Atmospheric Environment 44 (2010) 3719–3727

Contents lists available at ScienceDirect

Atmospheric Environment

journal homepage: www.elsevier.com/locate/atmosenv

Understanding of regional air pollution over China using CMAQ, part II. Process analysis and sensitivity of ozone and particulate matter to precursor emissions

Xiao-Huan Liu [a,b], Yang Zhang [a,*], Jia Xing [c], Qiang Zhang [d], Kai Wang [b], David G. Streets [d], Carey Jang [e], Wen-Xing Wang [a], Ji-Ming Hao [c]

[a] Shandong University, Jinan, Shandong Province 250100, P.R China
[b] North Carolina State University, Raleigh, NC 27695, USA
[c] Tsinghua University, Beijing 100084, P.R China
[d] Argonne National Laboratory, Argonne, IL 60439, USA
[e] The U.S. Environmental Protection Agency, Research Triangle Park, NC 27711, USA

ARTICLE INFO

Article history:
Received 10 December 2009
Received in revised form
26 March 2010
Accepted 29 March 2010

Keywords:
CMAQ
Process analysis
Indicators for O_3 and $PM_{2.5}$ chemistry
China

ABSTRACT

Following model evaluation in part I, this part II paper focuses on the process analysis and chemical regime analysis for the formation of ozone (O_3) and particulate matter with aerodynamic diameter less than or equal to 10 μm (PM_{10}) in China. The process analysis results show that horizontal transport is the main contributor to the accumulation of O_3 in Jan., Apr., and Oct., and gas-phase chemistry and vertical transport contribute to the production and accumulation of O_3 in Jul. Removal pathways of O_3 include vertical and horizontal transport, gas-phase chemistry, and cloud processes, depending on locations and seasons. PM_{10} is mainly produced by primary emissions and aerosol processes and removed by horizontal transport. Cloud processes could either decrease or increase PM_{10} concentrations, depending on locations and seasons. Among all indicators examined, the ratio of $P_{HNO_3}/P_{H_2O_2}$ provides the most robust indicator for O_3 chemistry, indicating a VOC-limited O_3 chemistry over most of the eastern China in Jan., NO_x-limited in Jul., and either VOC- or NO_x-limited in Apr. and Oct. O_3 chemistry is NO_x-limited in most central and western China and VOC-limited in major cities throughout the year. The adjusted gas ratio, AdjGR, indicates that PM formation in the eastern China is most sensitive to the emissions of SO_2 and may be more sensitive to emission reductions in NO_x than in NH_3. These results are fairly consistent with the responses of O_3 and $PM_{2.5}$ to the reductions of their precursor emissions predicted from sensitivity simulations. A 50% reduction of NO_x or AVOC emissions leads to a reduction of O_3 over the eastern China. Unlike the reduction of emissions of SO_2, NO_x, and NH_3 that leads to a decrease in PM_{10}, a 50% reduction of AVOC emissions increases PM_{10} levels. Such results indicate the complexity of O_3 and PM chemistry and a need for an integrated, region-specific emission control strategy with seasonal variations to effectively control both O_3 and $PM_{2.5}$ pollution in China.

1. Introduction

As a result of a fast economic development in China, increasingly high anthropogenic emissions of nitrogen oxides (NO_x), sulfur dioxide (SO_2), and volatile organic compounds (VOCs) lead to the multi-pollutant pollution with high concentrations of ozone (O_3) and particulate matter with aerodynamic diameters less than or equal to 10 μm (PM_{10}) (Zhang et al., 1998; Xu et al., 2006). Three-dimensional (3-D) air quality models provide a fundamental tool to simulate the linkages among meteorology, emissions, and air pollution. Understanding of such linkages and the formation mechanism of major pollutants such as O_3 and PM_{10} is critical to air quality management and climate change mitigation due to their important chemical and climatic impacts. Such linkages and mechanisms are often complex, involving various chemical and physical processes and multiphase reactions; therefore they rely on detailed process analyses using advanced tools such as the process analysis (PA) tool embedded in 3-D air quality models. PA in the U.S. EPA Community Multiscale Air Quality (CMAQ) is a tool that calculates

* Corresponding author at: Department of Marine, Earth, and Atmospheric Sciences, Campus Box 8208, NCSU, Raleigh, NC 27695, USA. Tel.: +1 919 515 9688; fax: +1 919 515 7802.
E-mail address: yang_zhang@ncsu.edu (Y. Zhang).

1352-2310/$ – see front matter © 2010 Elsevier Ltd. All rights reserved.
doi:10.1016/j.atmosenv.2010.03.036

integrated rate and mass changes of a reaction and a process, thereby providing valuable information to the development of the effective emission control strategies. Process analysis has been widely applied to study the fate and formation of gaseous and PM pollutants (e.g., Jang et al., 1995; Jiang et al., 2003; Hogrefe et al., 2005; Kwok et al., 2005; Zhang et al., 2005, 2009a; Kimura et al., 2008; Gonçalves et al., 2008; Tonse et al., 2008; Xu et al., 2008; Yu et al., 2009; Liu et al., in review).

A number of photochemical indicators have been developed to indicate the sensitivity of O_3 to changes in its precursors' emissions to assess the effectiveness of VOCs or NO_x emission controls in reducing O_3 (e.g., Sillman, 1995; Tonnesen and Dennis, 2000a,b; Zhang et al., 2009a). One of the indicators, i.e., the ratio of the production of hydrogen peroxide (H_2O_2) and nitrate acid (HNO_3), can be determined through the PA tool. In this Part II paper, the PA tool embedded in CMAQ is used to identify the most influential processes and chemical reactions that lead to the formation and accumulation of surface O_3, PM_{10}, and components of PM_{10} such as SO_4^{2-}, NO_3^-, and SOA in China in Jan., Apr., Jul., and Oct. 2008. The PA products (e.g., odd oxygen production, OH chain length) provide the characteristics of spatial and seasonal variations of the total oxidation capacity over China. The ratios of $P_{H_2O_2}/P_{HNO_3}$ combined with several other photochemical indicators are used to indicate the NO_x vs. VOC-limited O_3 chemistry in China, which is further verified through sensitivity simulations. Several indicators for PM chemistry and additional sensitivity simulations with different emission reduction scenarios are used to examine the sensitivity of PM formation to changes in its precursor emissions. Such information provides useful perspectives for the development of local and regional emission control strategies and/or assessing their effectiveness over space and time in China.

2. Methodology for process analysis

PA embedded in CMAQ includes the Integrated Process Rates (IPR) that can identify dominant physical processes for O_3 and PM_{10} and the Integrated Reaction Rates (IRR) that can determine the most influential reactions for their precursors in the gas phase and the chemical regime for O_3 chemistry. Hourly IPRs for 33 species and IRRs for 187 gas-phase reactions in the 2005 Carbon Bond Mechanism (CB05) are calculated in the 4-month simulations at 36-km. The hourly IPRs are analyzed for major pollutants in the planetary boundary layer (PBL) (~0–2.9 km, corresponding to layers 1–10) to examine the relative importance of major atmospheric processes such as the emissions of primary species, horizontal transport, vertical transport, gas-phase chemistry, dry deposition, cloud processes, and aerosol processes. Horizontal transport is the sum of horizontal advection and diffusion, and vertical transport is the sum of vertical advection and diffusion. Aerosol processes represent the net effect of aerosol thermodynamics, new particle formation, condensation of sulfuric acid and organic carbon on preexisting particles, and coagulation within and between Aitken and accumulation modes of PM. Cloud processes represent the net effect of cloud attenuation of photolytic rates, aqueous-phase chemistry, below- and in-cloud mixing with chemical species, cloud scavenging, and wet deposition. The IPR results for O_3, PM_{10}, SO_4^{2-}, NO_3^-, and SOA are analyzed at 8 sites including 5 urban sites (Beijing, Shanghai, Guangzhou, Chengdu, and Jinan), 1 mountain site (Mt. Tai located in the North China Plain), 1 rural site (Xiaoping), and 1 background site (Waliguan). The main characteristics of these sites are described in the Supplementary information. The IRRs of 187 reactions are grouped into 34 products according to the reactions for radical initiation, propagation, production, and termination (see Table 1 in Zhang et al., 2009b). The grouping is based on the method used for CBM-IV in CMAQ (Byun and Ching, 1999) but modified for CB05 in this work. In this paper, the chemical production of total odd oxygen (Total_OxProd) (where $O_x = O_3$ + nitrogen dioxide (NO_2) + 2 × nitrogen trioxide (NO_3) + oxygen atom (O) + excited-state oxygen atom (O^1D) + peroxyacyl nitrate (PAN) + 3 × dinitrogen pentoxide (N_2O_5) + nitric acid (HNO_3) + pernitric acid (HNO_4) + unknown organic nitrate) that influences tropospheric oxidation capacity is examined. The chain length of hydroxyl radical (OH) (OH_CL) is the average number of times a newly-created OH radical will be recreated through radical chain propagation before it can be removed from the cycle (Seinfeld and Pandis, 2006). OH_CL provides a measure of an overall oxidation efficiency of the atmosphere (Zhang et al., 2009a). The ratio of production rates of hydrogen peroxide (H_2O_2) and nitric acid (HNO_3) ($P_{HNO_3}/P_{H_2O_2}$) from the IRR results (where P_{HNO_3} is the sum of HNO_3 production via reactions OH + NO_2, NO_3 + HC, and N_2O_5 hydrolysis) is used to decide the VOC- or NO_x-limited nature of O_3 chemistry at a given site during different seasons and whether the model is correctly predicting the responses of O_3 to VOC and/or NO_x emission controls. In addition to $P_{HNO_3}/P_{H_2O_2}$ from IRR output, several additional indicator species are calculated to determine O_3 chemistry. These include NO_y, the ratios of H_2O_2/HNO_3, $H_2O_2/(O_3 + HNO_3)$, O_3/NO_x, O_3/NO_y, HCHO/NO_2 and HCHO/NO_y (Lu and Chang, 1998; Sillman, 1995; Sillman et al., 1997; Sillman and He, 2002; Zhang et al., 2009a,b). Three indicators: the degree of sulfate neutralization (DSN), gas ratio (GR), and adjusted gas ratio (AdjGR) are used to determine the sensitivity of PM formation. Their definitions and theoretical basis for both O_3 and PM chemistry indicators are provided in Table 2 in Zhang et al. (2009b) and references therein.

3. Results from process analysis

3.1. Analyses of Integrated Process Rates (IPR) in the PBL

Figs. 1 and 2 show the daily-mean hourly contributions of individual processes averaged in the PBL to the concentrations of O_3 and PM_{10}, respectively, at 3 sites: Beijing, Guangzhou, and Mt. Tai. Horizontal transport plays a dominant role in the accumulation of O_3 in Jan., Apr., and Oct., and gas-phase chemistry and vertical transport contribute to the production and accumulation of O_3 in Jul. at all sites. O_3 at Beijing is vented out of the PBL mainly through vertical transport and destroyed via NO titration in Jan., Apr., and Oct. and vented out via horizontal transport in Jul. O_3 at Guangzhou is mainly destroyed via NO titration in Jan., Apr., and Oct. and vented out through both horizontal and vertical transport in Jul. At Mt. Tai, the main processes contributing to O_3 loss may include vertical transport and gas-phase chemistry in Jan. and Apr. and horizontal transport and cloud processes in Jul. and Oct.

Local primary emissions or emissions from upwind areas are the dominant contributor to PM_{10} concentrations at all urban and mountain sites in all months (Fig. 2). A higher contribution of primary emissions at Guangzhou indicates that PM_{10} is composed mainly of primary PM at Guangzhou, which is different from that at the other two sites where both primary and secondary PM are important components. PM_{10} can be formed via aerosol processes such as homogeneous nucleation and condensation at all sites in all months except during some days in Jan. and Apr. at Guangzhou where NaCl is neutralized by large amounts of HNO_3 to release Cl^- from the particulate phase to the gas phase, causing a net loss of PM mass due to this gas/aerosol re-partitioning process. While cloud processes can increase PM_{10} formation due to the aqueous-phase oxidation of SO_2 during most days in Guangzhou in Jan. and Apr., they can also lead to a decrease in PM_{10} formation on some days at Guangzhou and other sites due to a dominance of cloud scavenging. Horizontal transport provides the main sink for PM_{10} at all sites in all months. Vertical transport may either serve as a sink or a source for PM_{10} accumulation.

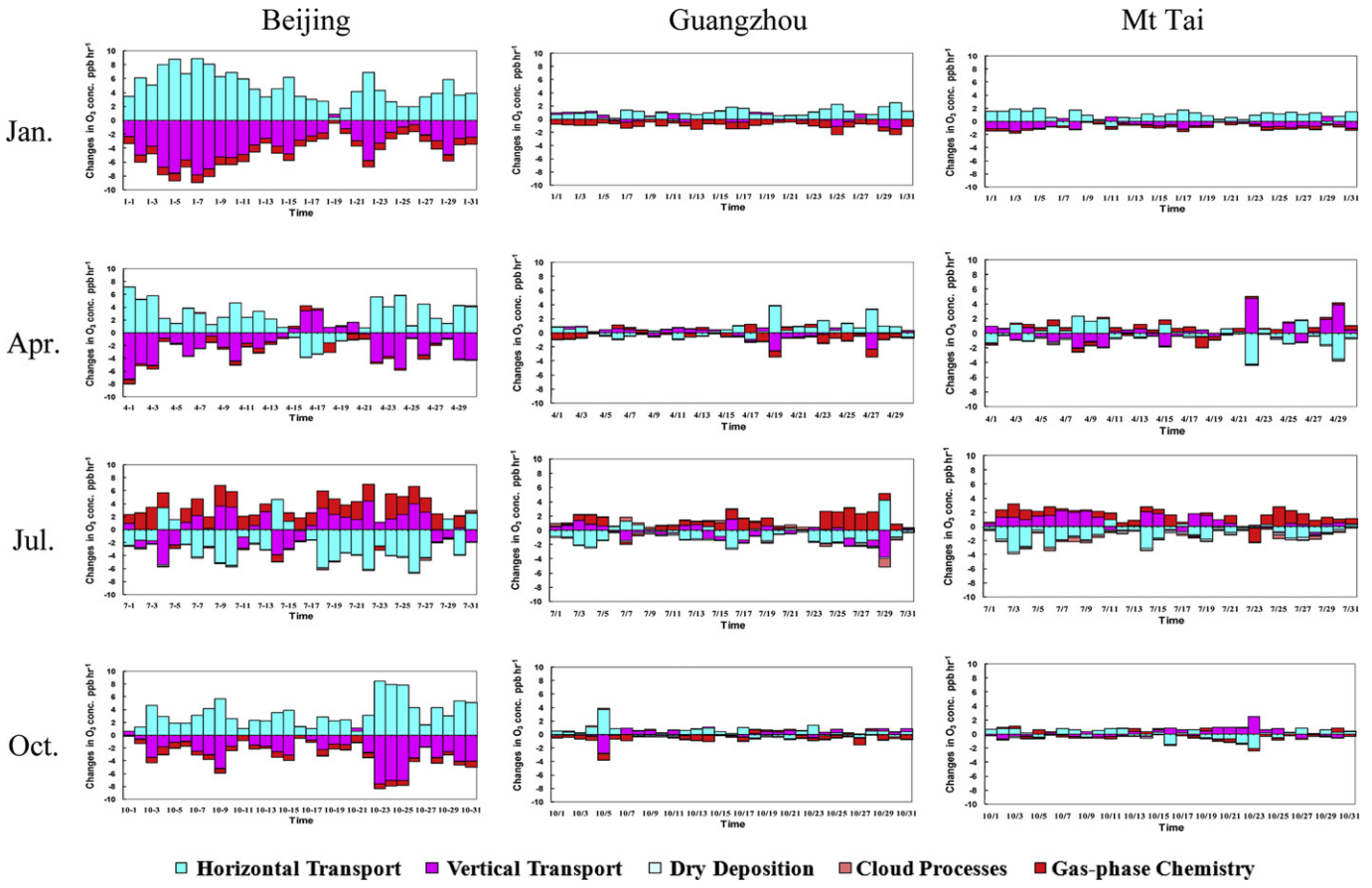

Fig. 1. Daily-mean hourly contributions of individual processes to the mixing ratios of O_3 in the PBL (0–2.9 km) at 3 sites (Beijing, Guangzhou, and Mt. Tai) in China in 2008.

Secondary aerosols are an important contributor to regional haze in China. Figures S-1–S-3 show daily-mean contributions of individual chemical and physical processes to SO_4^{2-}, NO_3^-, and SOA, respectively, at the 3 sites. The main processes contributing to the production/accumulation of SO_4^{2-} include cloud processes and emissions at Guangzhou in all months, cloud and aerosol processes at Mt. Tai in all months and at Beijing in Apr. and Jul., and emissions and horizontal transport at Beijing in Jan. and Oct. Horizontal transport is the dominant processes contributing to the depletion of SO_4^{2-} at Guangzhou and Mt. Tai in all months and at Beijing in Apr. and Jul. Vertical transport dominates the sink of SO_4^{2-} at Beijing on most of days in Jan. and Oct. NO_3^- and SOA concentrations at Beijing, Guangzhou, and Mt. Tai are enhanced primarily by aerosol processes in all months. Their loss is mainly caused by horizontal transport at these sites.

Figure S-4 contrasts the monthly-mean contributions of each process to O_3 and PM_{10} concentrations in different layers in the PBL and one layer above PBL (layer 10, ~2900 m) at one urban site (i.e., Beijing) and on rural site (i.e., Xiaoping) during summer. At Beijing, horizontal transport and vertical transport are the main sources of O_3 accumulation, and dry deposition and gas-phase chemistry are the main sinks of O_3 below layer 3 (surface to ~150 m). O_3 at layers ≥3 (~150–2000 m) mainly comes from gas-phase chemistry production, and horizontal transport contributes negatively from layer 4 to the top of PBL. The contribution of vertical transport to O_3 mixing ratios at different layers may either be negative or positive. The cloud processes contribute slightly to the O_3 increase below 650 m via convective mixing process that brings high O_3 aloft to lower atmosphere and to the O_3 loss near the top of PBL via cloud attenuation of photolytic rates and scavenging and wet deposition processes. As compared with Beijing, horizontal transport contributes to the accumulation of O_3 and vertical transport contributes to the loss of O_3 at higher altitudes (layers 1–7) and gas-phase chemistry contributes to O_3 production in all layers except for layer 10 at Xiaoping. At Beijing, PM_{10} comes from local emissions mainly below 300 m, horizontal transport helps transport particles from heavily-polluted areas to downwind areas, particularly between 150 and 300 m. Particles below ~74 m are also significantly uplifted to higher layers (100–700 m) via vertical transport, which is the opposite to its contribution to surface and near-surface O_3. PM_{10} is mainly produced via aerosol processes in the upper layers (>~450 m) where low temperatures favor the formation of its secondary components. Significant loss of PM_{10} due to aerosol processes occur at heights below 450 m but the net layer-weighted contribution of aerosol processes in the PBL is positive (see Fig. 2), indicating a net production of PM_{10} due to aerosol processes. Dry deposition is the main sink of PM_{10} at surface. Cloud processes contribute slightly to PM_{10} removal under ~1500 m. As compared with Beijing, horizontal transport contributes to the accumulation of PM_{10} and vertical transport contributes to its loss for layers 1–8, PM processes contribute to PM_{10} production in layers 1–2, 5, and 10, and cloud processes contribute to PM_{10} loss in all layers at Xiaoping. These results illustrate roles of various processes at different heights at different sites.

3.2. Integrated Reaction Rates (IRRs) and additional indicator analyses

3.2.1. IRR results

Fig. 3 shows the spatial distributions of monthly-mean total O_x chemical production rates, OH chain length, and the amount of OH reacted with anthropogenic and biogenic VOCs (AVOCs and BVOCs)

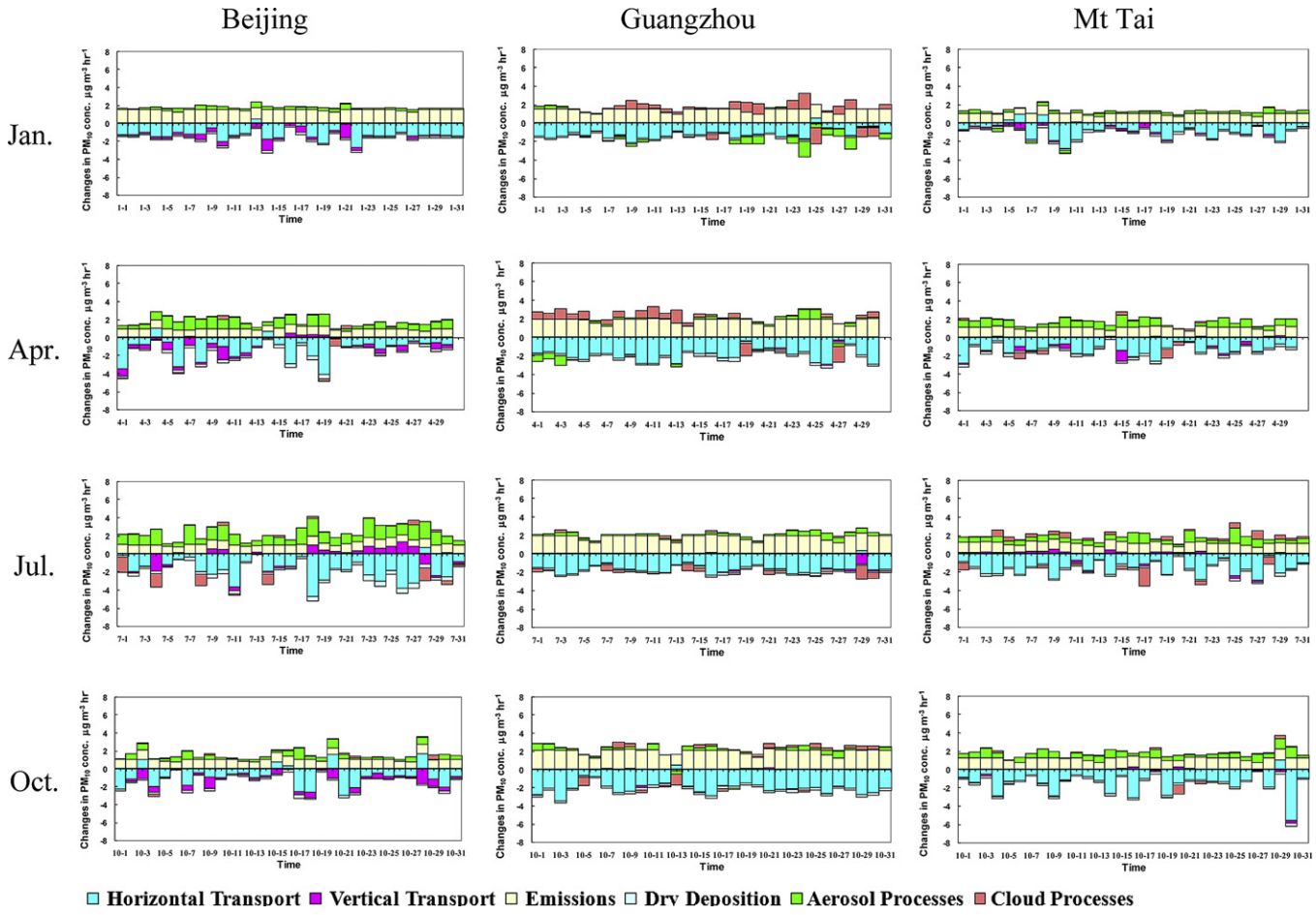

Fig. 2. Daily-mean hourly contributions of individual processes to the mass concentrations of PM_{10} in the PBL (0–2.9 km) at 3 sites (Beijing, Guangzhou, and Mt. Tai) in China in 2008.

over East Asia in the four months. Significant O_x production occurs over the eastern China throughout the year, indicating a stronger oxidation capacity over relatively-developed areas as compared with the central and western China. The O_x production is stronger over South China than North China due to a stronger solar radiation. The strongest oxidation capacity occurs during summer and the weakest during winter. By contrast, OH chain length shows the largest values in Jan. and the lowest in Jul., indicating a faster removal of OH from the photochemical reaction cycles during summer due to stronger oxidation rates of VOCs by OH radicals. Higher reaction rates of OH with AVOCs and BVOCs occur in summer. AVOCs are significant in the North China Plain and PRD areas where AVOC emissions are high due to dense population and rapid economic growth and BVOC emissions are relatively low due to fewer vegetations and a dry weather. BVOCs reacted with OH radicals are typically significant in the southeastern China where the vegetation coverage is dense and BVOC emissions are high. Figure S-5 compares these IRR products at 8 sites. Total O_x production is the highest in Jul. at all sites. The oxidation capacities in Apr. and Oct. are quite similar at all sites. The O_x production at urban sites, e.g., Beijing and Shanghai, are much higher than rural sites, especially in Jul., indicating that the precursor concentrations are another key factor that influences O_3 formation, in addition to solar radiation. The OH chain length shows the largest values in Jan. and the lowest in Jul. at all sites except at Guangzhou where the maximum OH chain length occurs in Jul. and the minimum occurs in Apr., with a stronger seasonal variation at rural and background sites. The rates of OH reacted with AVOCs (OH_AVOC) are significantly higher at urban sites than those at rural sites due to higher AVOC emissions in urban areas. OH amounts reacted with BVOCs (OH_BVOC) at the rural site (e.g., Xiaoping) are equal to or slightly higher than those in urban areas (e.g., Beijing, Shanghai), due to higher BVOC emissions in the rural areas. OH_ AVOCs are significantly higher than OH_BVOCs in urban areas but slightly higher or even lower than OH_BVOCs at rural sites in Jul., consistent with the findings of Zhang et al. (2009a).

3.2.2. *Analysis of chemical indicators and sensitivity of model predictions to emissions*

Fig. 4 shows the spatial distributions of monthly-mean values of $P_{H_2O_2}/P_{HNO_3}$ from the IRR output during the afternoon time (from 1 pm to 6 pm, local time) in the four months. The values of $P_{H_2O_2}/P_{HNO_3}$ less than 0.2 indicate a VOC-limited chemistry and higher values indicate a NO_x-limited chemistry (Tonnesen and Dennis, 2000b). In Jan., the ratios of $P_{H_2O_2}/P_{HNO_3}$ are below 0.2 over the northeastern China, North China plain, the YRD and PRD areas, and several big cities through China, indicating a VOC-limited O_3 atmosphere in the developed area of China where NO_x emissions from traffic and industry activities are high and vegetations are sparse, whereas other areas are in a regime with NO_x-limited O_3 chemistry due to the large amount of trees that produce high levels of BVOCs or less NO_x emissions into the atmosphere. In Jul., most of these VOC-limited areas change to NO_x-limited, although some urban areas (e.g., Beijing, Tianjin, Shanghai) remain to be VOC-limited, due to significantly higher NO_x emissions caused by power

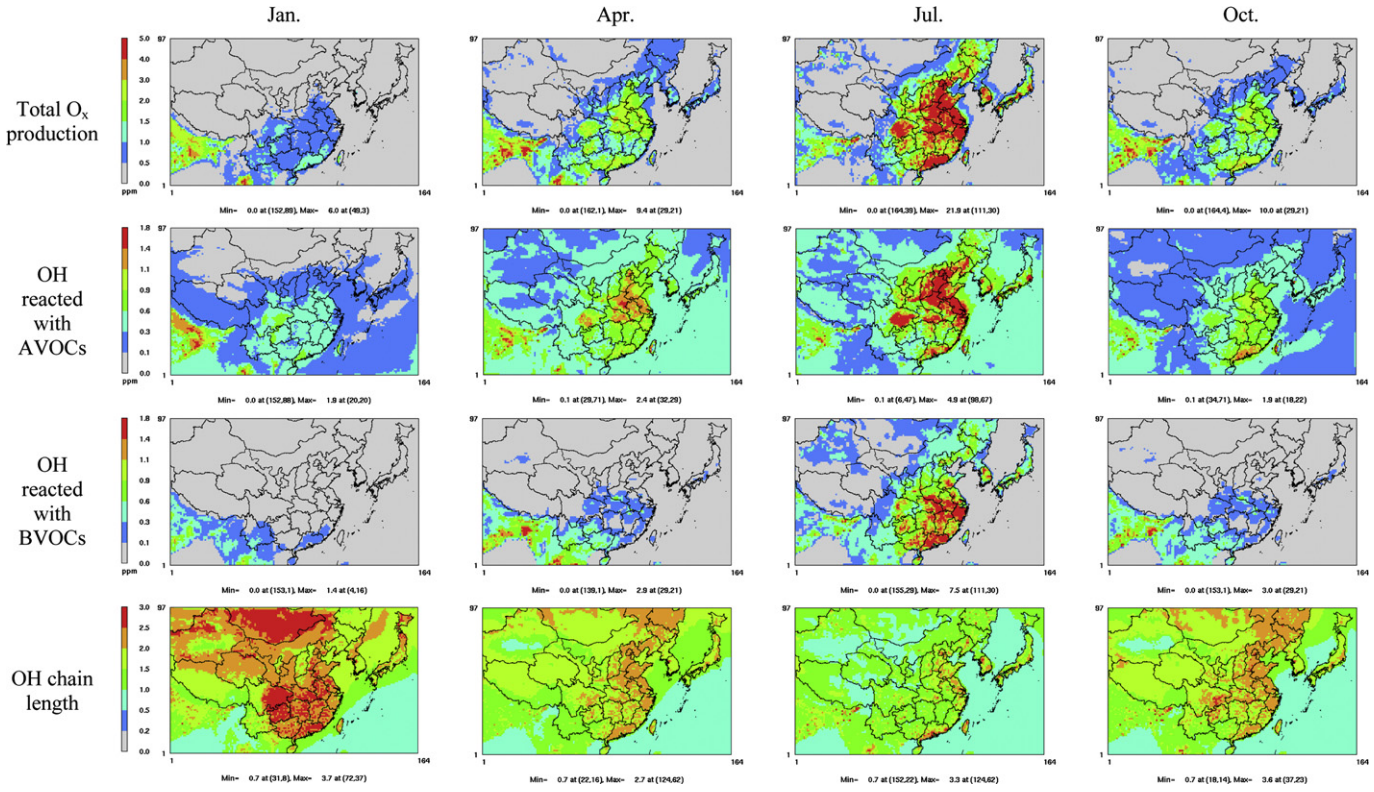

Fig. 3. Spatial distributions of total O_x production, OH chain length and OH reacted with AVOCs and BVOCs at surface in China in 2008.

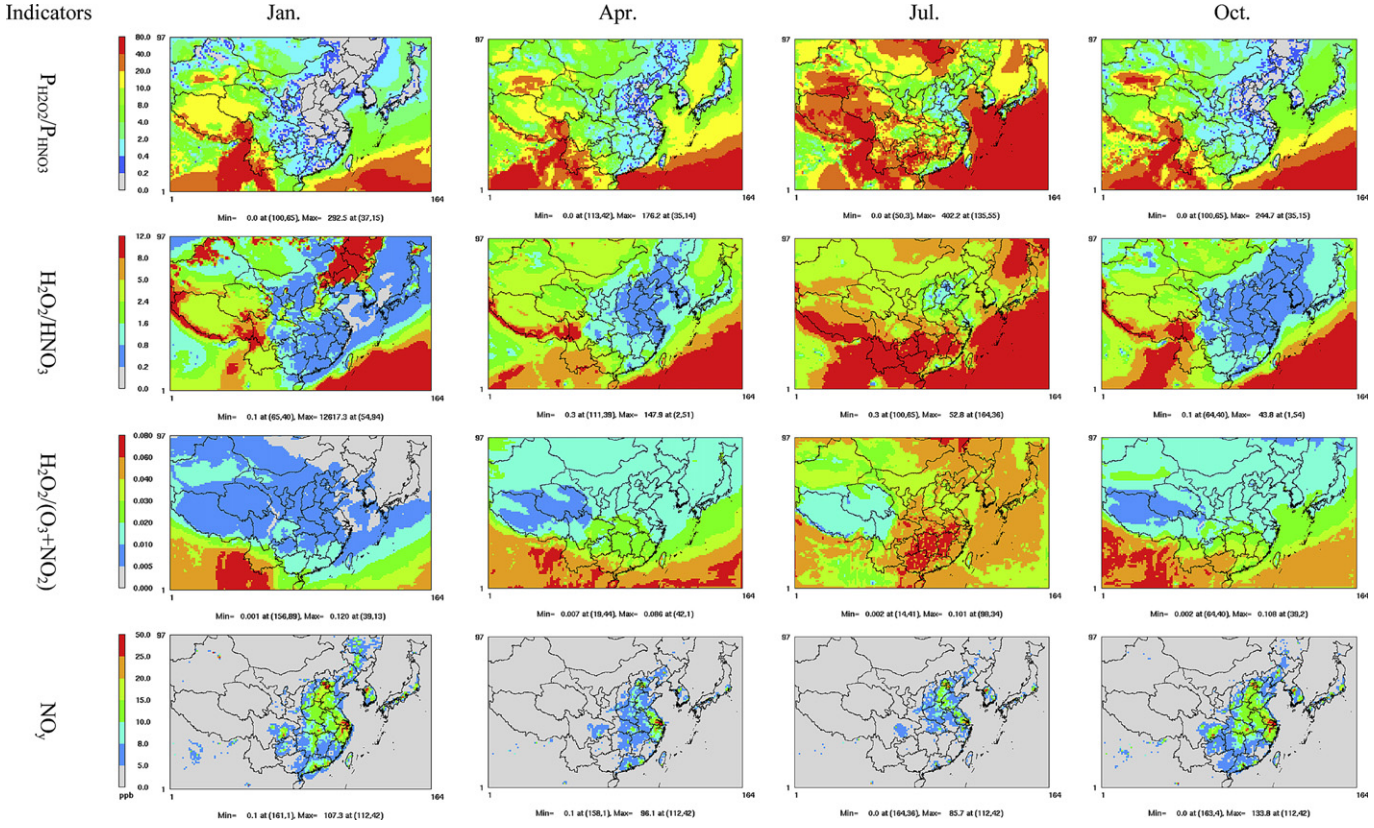

Fig. 4. Spatial distribution of monthly-mean ratios of $P_{H_2O_2}/P_{HNO_3}$, H_2O_2/HNO_3, $H_2O_2/(O_3 + NO_2)$, NO_y, O_3/NO_x, O_3/NO_y, HCHO/NO_2, and HCHO/NO_y during afternoon (1–6 pm, local time) at surface in China in 2008.

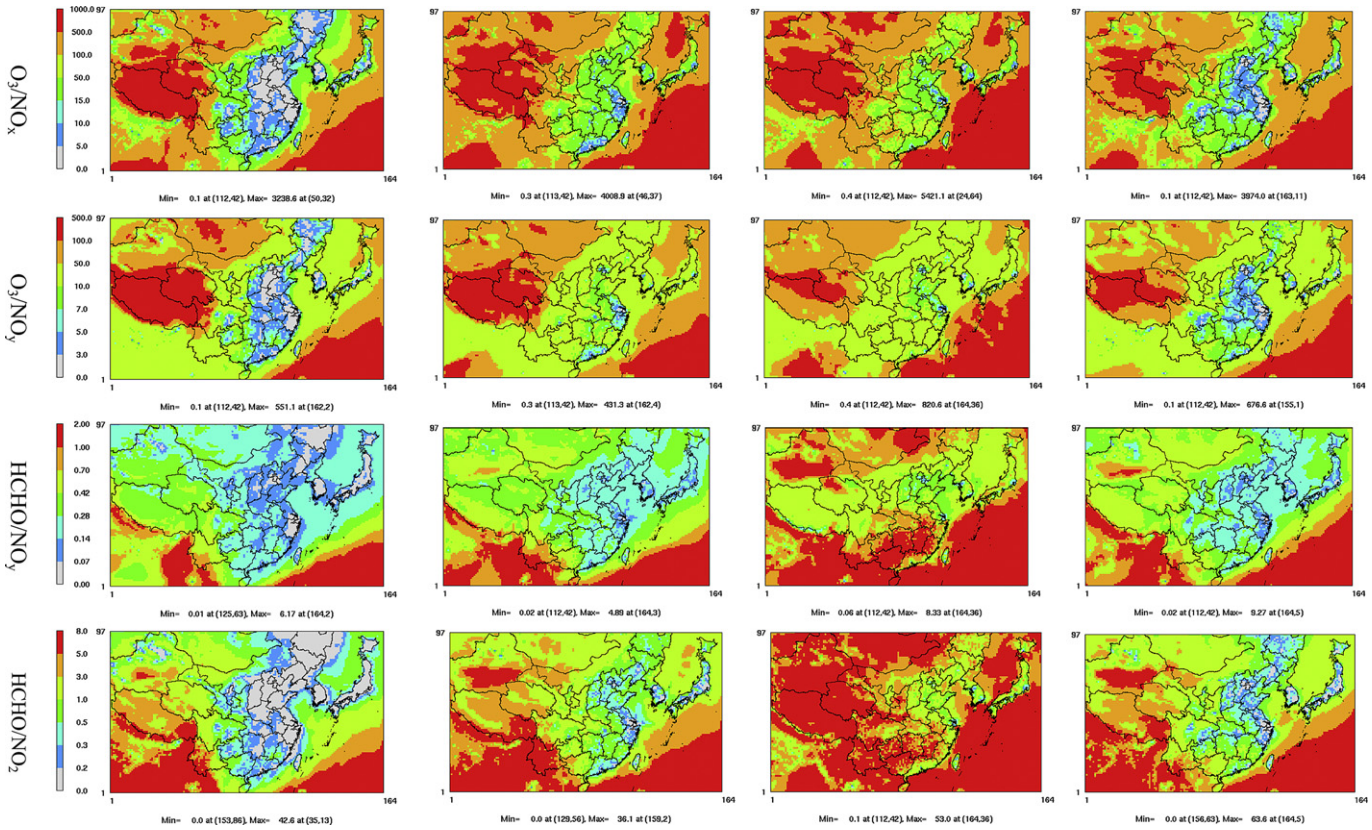

Fig. 4. (*continued*).

plants and vehicles over those areas. The values of $P_{H_2O_2}/P_{HNO_3}$ over the eastern portion of the domain in Apr. and Oct. are mostly higher than 0.2 except for the large metropolitan areas in the northeastern China, South Korea, and Japan.

Since $P_{H_2O_2}/P_{HNO_3}$ was developed based on model simulations over North America, two sensitivity simulations are conducted over China in Jul. 2008 to verify the results based on $P_{H_2O_2}/P_{HNO_3}$, one with a 50% reduction in domain-wide NO_x emissions, and one with a 50% reduction in AVOCs emissions. The absolute and percentage differences in simulated O_3 mixing ratios are shown in Fig. S-6. Reduction of emissions of AVOCs leads to an O_3 decrease over the central and eastern China, with 5–13% decrease over the North China Plain. NO_x reduction leads to a larger O_3 decrease over much larger areas, with the largest reduction of 16.3 ppb and 27.7% domain-wide. The larger response of O_3 to reduction of NO_x emissions than the reduction of AVOCs emissions indicates a NO_x-limited O_3 chemistry in most areas in July, consistent with the results using $P_{H_2O_2}/P_{HNO_3}$. O_3 increase is found over several large cities (i.e., cities located in the North China Plain, YRD, PRD, Taiwan, South Korea, and Japan), indicating that O_3 chemistry in these areas is VOC-limited, which is also consistent with the results based on the ratios of $P_{H_2O_2}/P_{HNO_3}$.

While $P_{H_2O_2}/P_{HNO_3}$ is a robust indicator for O_3 chemistry, other indicators such as the values of H_2O_2/HNO_3, $H_2O_2/(O_3 + NO_2)$, NO_y, O_3/NO_x, O_3/NO_y, $HCHO/NO_y$, and $HCHO/NO_2$ in the afternoon can also serve as effective indicators for O_3 chemistry (Tonnesen and Dennis, 2000b; Zhang et al., 2009a,b). The transition values are 0.2 for H_2O_2/HNO_3 (Lu and Chang, 1998; Sillman, 1995; Sillman et al., 1997; Tonnesen and Dennis, 2000b), 0.02 for $H_2O_2/(O_3 + NO_2)$ (Tonnesen and Dennis, 2000b), 20 for NO_y (Lu and Chang, 1998; Sillman, 1995), 15 for O_3/NO_x (Tonnesen and Dennis, 2000a,b), 7 for O_3/NO_y (Sillman et al., 1997), 0.28 for $HCHO/NO_y$ (Lu and Chang, 1998; Sillman, 1995), and 1 for $HCHO/NO_2$ (Tonnesen and Dennis, 2000b). Values less than these transition values indicate a VOC-limited chemistry and higher values indicate a NO_x-limited chemistry for all the above indicators except NO_y (for NO_y, a value greater than 20 means VOC-sensitive condition, otherwise NO_x chemistry).

As shown in Fig. 4, the values of $H_2O_2/(O_3 + NO_2)$, O_3/NO_x, O_3/NO_y, $HCHO/NO_y$ and $HCHO/NO_2$ over the eastern China in Jan. are all smaller than their receptive transition values, indicating a VOC-limited O_3 chemistry, which is consistent with the results based on the ratios of $P_{H_2O_2}/P_{HNO_3}$. Based on the transition values proposed by the original developers, however, some of these indicators, i.e., $H_2O_2/(O_3 + NO_2)$, $HCHO/NO_y$, and $HCHO/NO_2$ indicate larger areas under the VOC-limited condition as compared with those indicated by $P_{H_2O_2}/P_{HNO_3}$. The values of NO_y show that the NO_y concentrations larger than 20 ppb occur only in the areas surrounding Beijing, Tianjin, and Shanghai, indicating VOC-limited areas that are much smaller than those indicated by $P_{H_2O_2}/P_{HNO_3}$. The VOC-limited areas with an adjusted threshold value of NO_y of 5 ppb by Zhang et al. (2009a) are much more consistent with those indicated by $P_{H_2O_2}/P_{HNO_3}$. The ratios of H_2O_2/HNO_3 in Jan. are higher than 0.2 (indicating a NO_x-limited chemistry) over almost the entire domain, which is also inconsistent with $P_{H_2O_2}/P_{HNO_3}$. Five indicators (i.e., NO_y, O_3/NO_x, O_3/NO_y, $HCHO/NO_2$, and $HCHO/NO_y$) show results consistent with $P_{H_2O_2}/P_{HNO_3}$ in Jul., a NO_x-limited chemistry over nearly the entire China but a VOC-limited chemistry over several large cities. The ratios of H_2O_2/HNO_3 indicate a NO_x-limited O_3 chemistry over China including several big cities (e.g., Beijing) where a VOC-limited regime is denoted by $P_{H_2O_2}/P_{HNO_3}$ and the 5 indicators above. An adjusted value of 2.4 for H_2O_2/HNO_3 proposed by Zhang et al. (2009a) will, however, indicate a VOC-limited chemistry over those metropolitan areas. $H_2O_2/(O_3 + NO_2)$ indicates that O_3 chemistry is NO_x-limited over large cities and a VOC-limited over the Qinghai-Tibet Plateau in Jul., both are inconsistent with the results based on $P_{H_2O_2}/P_{HNO_3}$.

These results show that the transition values originally proposed by developers may not always be valid in China, due to several factors. For example, some of the original transition values were developed based on limited field measurements (Zhang et al., 2009b) or model simulations with different mechanisms and horizontal grid resolutions (Sillman and He, 2002; Wang et al., 2005; Zhang et al., 2009b). Furthermore, none of these indicators are based on observations or model simulations over China. These factors warrant a need to adjust the transition values of these indicators to better fit the atmospheric conditions in China. Zhang et al. (2009b) examined the robustness of those indicators through a full-year simulation over the North America and suggested adjusting the transition values of $H_2O_2/(O_3 + NO_2)$ from 0.02 to 0.04 in summer, H_2O_2/HNO_3 from 0.2 to 2.4, NO_y from 20 to 5, O_3/NO_x from 15 to 60, and O_3/NO_y from 7 to 15 in Jan. and Aug. Based on the simulated spatial distribution of H_2O_2/HNO_3 in Jan., the adjusted transition value of 2.4 based on North American conditions would not give VOC-limited condition over both the eastern China and the North China Plain and NO_x-limited chemistry over the western China; however adjusting H_2O_2/HNO_3 from 0.2 to 1.6 would work in Jul. For indicator $H_2O_2/(O_3 + NO_2)$, adjusting transition value does not work in either Jan. or Jul., indicating that this indicator may not be applicable for China. For other indicators, adjusting transition value from 20 to 5 for NO_y, from 0.28 to 0.14 for HCHO/NO_y, and from 1 to 0.3 in Jan., Apr., and Oct. and 0.5 in Jul. for HCHO/NO_2 will allow these indicators to predict an O_3 sensitivity that is more consistent with that predicted by $P_{H_2O_2}/P_{HNO_3}$.

Fig. 5 shows spatial distributions of three PM chemistry indicators including the degree of sulfate neutralization (DSN), gas ratio (GR), and adjusted gas ratio (AdjGR) for sensitivity of $PM_{2.5}$ formation to its precursors. Full sulfate neutralization with DSN ≥ 2 occurs largely in some areas in the eastern China in all months with the smallest areas in July, implying NH_4NO_3 formation over those areas. As indicated in Zhang et al. (2009b), however, a transition value of 1.5 for DSN is more appropriate than a value of 2 to indicate the formation of NH_4NO_3 because of a strong thermodynamic affinity between NH_4^+ and NO_3^- in winter and the lack of sufficient SO_4^{2-} to neutralize excess NH_3, in some areas in summer. Values of GR >1, 0–1, and <0 indicate NH_3-rich, neutral, and poor conditions, respectively. NH_3-rich condition occurs in much larger areas in Apr., Jul., and Oct. than in Jan. due to high NH_3 emissions, whereas NH_3-poor condition occurs only over a small area in the northwestern China and oceanic areas. The full neutralization assumed in GR deviation may underestimate the amount of free NH_3 and thus NH_4NO_3, particularly under the winter condition when such an assumption may not hold. This limitation is overcome by defining DSN and using it to correct GR as an adjusted GR (i.e., AdjGR, see equations (7)–(9), Zhang et al., 2009b). Compared with GR, all areas with GR < 1 now have AdjGR ≥ 1 in all four months, reflecting a greater potential for NH_4NO_3 formation over those areas, which is more consistent with the adjusted DSN value to indicate NH_4NO_3 formation. High values of GR and AdjGR in the southern and eastern China in Jul. are due to very small molar concentrations of total nitrate (TNO_3, which is the total molar concentration of NO_3^- and HNO_3) in the denominator.

Based on Ansari and Pandis (1998) and the definition of the AdjGR, for areas with AdjGR > 1 (i.e., most eastern and southern China), NH_3 is rich and sulfate is poor; PM formation is sensitive to the emissions of its major precursors including SO_2, NO_x, and NH_3, in particular, SO_2. In those areas, NO_3^- is more sensitive to changes in TNO_3 than in NH_3 because of abundance of free NH_3. Fig. S-7 shows the sensitivity of PM_{10} to 50% reduction of emissions of SO_2, NO_x, NH_3, and AVOCs. PM_{10} concentrations decrease due to SO_2 emission reduction by up to -27.8% (or -11.5 μg m^{-3}), NO_x emission reduction by up to -24.9% (or -17.5 μg m^{-3}), and NH_3 emission reduction by up to -16.8% (or -10.8 μg m^{-3}). While PM_{10} concentrations in some areas in the northern China (e.g., Beijing, Tianjin, Shangdong Province) are equally sensitive to emission reductions for SO_2 and NO_x, other regions are more sensitive to the reduction of SO_2 emissions (by -27.8% to -9% vs. -6%–0%). A 50% reduction of NO_x emissions leads to a larger percentage decrease in PM_{10} than a 50% reduction of NH_3 emissions (by -25.0% to -9% vs. -16.8% to -6%). These results are fairly consistent with the results indicated by AdjGR. AVOCs emission reduction in Jul. over the entire domain results in higher PM_{10} concentrations over developed areas up to 3.5 μg m^{-3} and 8.8%, due to an increase in the concentrations of the secondary PM species such as SO_4^{2-} and NO_3^- when more OH radicals become available for the oxidation of SO_2 and NO_x. Although the treatments of SOA formation are somewhat incomplete and also uncertain in CMAQ, the simulated

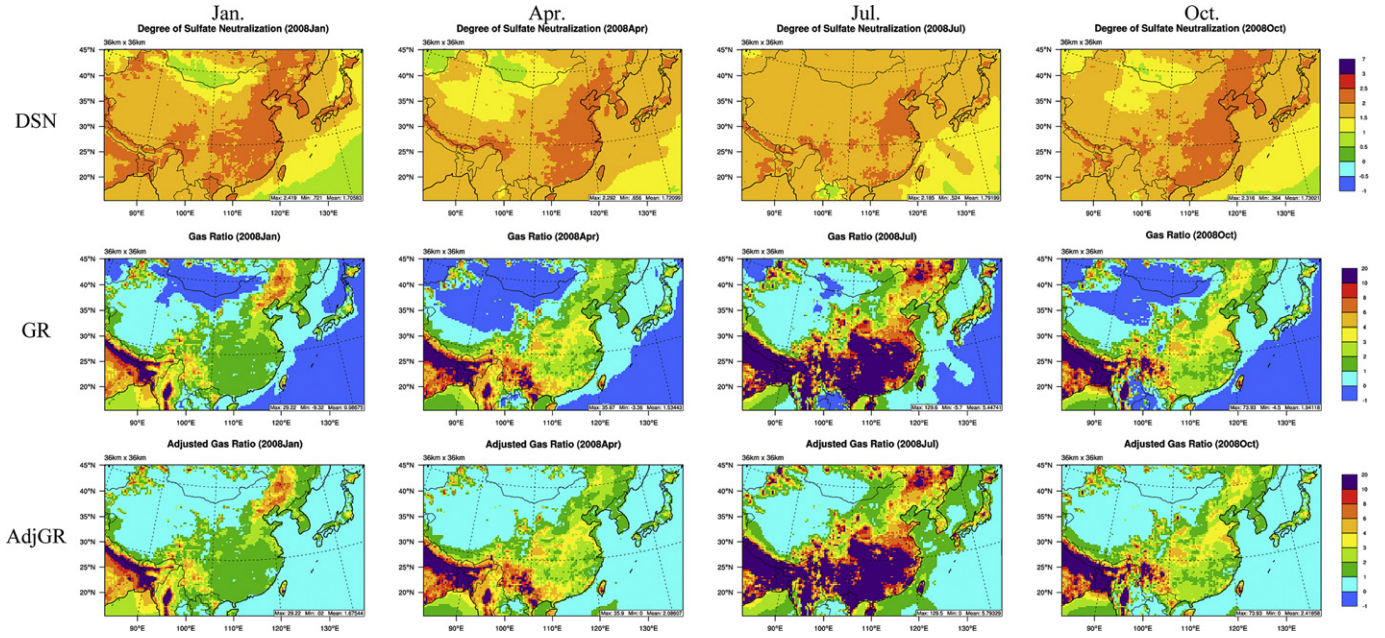

Fig. 5. Spatial distribution of the degree of sulfate neutralization (DSN), gas ratio (GR), and adjusted gas ratio (AdjGR) in China in 2008.

impact of AVOCs on O_3 and PM_{10} in this study are consistent with findings of Meng et al. (1997) and Pai et al. (2000) who reported that a 50% reduction in AVOC emissions may decrease O_3 by 31–34% but increase PM formation by 1–19% through increasing particulate nitrate formation in California, U.S. The sensitivity simulation results indicate that controlling SO_2 emission will be the most effective strategy to reduce PM_{10} pollution in most areas in July and additional control of emissions of NO_x and NH_3 can further reduce PM formation in the northern China, whereas controlling SOA precursors may lead to an enhanced PM formation, thus dis-benefiting the integrated control of ambient O_3 and PM_{10}.

4. Conclusions

The IPR and IRR embedded in CMAQ are applied to quantify the contributions of individual atmospheric processes to the formation and distributions of major pollutants and their seasonal variations in China in Jan., Apr., Jul., and Oct. 2008. The indicators for O_3 and PM chemistry are examined to understand their formation mechanisms via chemical transformations and provide a theoretical basis for the development of the integrated emission control strategies for their dominant precursors. The IPR analysis suggests that horizontal transport is a main process for the accumulation of O_3 in Jan., Apr., and Oct., and gas-phase chemistry and vertical transport contribute to the production and accumulation of O_3 in Jul. at all sites. O_3 can be removed through vertical and horizontal transport, gas-phase chemistry, and cloud processes, depending on locations and seasons. Primary emissions in local or upwind areas and aerosol processes are the main sources of PM_{10} and horizontal transport removes PM_{10} at all sites. Cloud processes could help decrease or increase PM_{10} concentrations, depending on locations and seasons. Cloud and aerosol processes are the dominant processes contributing to the formation of SO_4^{2-} and NO_3^-. Aerosol processes and in some cases vertical and horizontal transport contribute to the SOA production. The IRR results show that the strongest and weakest oxidation capacities occur in summer and winter, respectively, and a stronger O_x production is found over the eastern China than that over the central and western China. OH reacted with VOCs is the highest during summer and the lowest in winter, and OH mainly reacted with AVOCs in urban areas whereas such rates are typically slightly higher or even lower than those of OH with BVOCs at rural sites.

The ratios of $P_{H_2O_2}/P_{HNO_3}$ indicate a NO_x-limited O_3 chemistry over almost entire China during summer except several metropolitan areas, which changes to VOC-limited chemistry over the eastern China, as well as some major cities in most provinces under the cold weather in winter. Some provinces such as Shandong, Henan, and Jiangsu in the North Chain plain experience a transition from VOC-limited in Jan. to NO_x-limited conditions in Apr. and from NO_x-limited in Jul. back to VOC-limited conditions in Oct. Several megacities such as Beijing, Shanghai, Tianjin, and cities in the YRD and PRD areas are always under the VOC-limited conditions throughout the entire year due to large amounts of traffic and industrial emissions of NO_x. These results are consistent with results from two sensitivity simulations: one with a 50% reduction of NO_x emissions and the other with a 50% reduction of AVOC emissions in Jul., indicating the robustness of using the ratio of $P_{H_2O_2}/P_{HNO_3}$ to indicate O_3 chemistry regimes in China. The transition values originally proposed by the developers may not directly be applicable to China. They would need to be adjusted from 0.2 to 1.6 for H_2O_2/HNO_3 in winter, from 20 to 5 for NO_y, from 0.28 to 0.14 for $HCHO/NO_y$, and from 1 to 0.3 in Jan., Apr., and Oct. and from 1 to 0.5 in Jul. for $HCHO/NO_2$ to bring O_3 chemistry regimes more inline with results based on $P_{H_2O_2}/P_{HNO_3}$. Compared with GR, the adjGR provides a more robust indicator for PM chemistry regime. The AdjGR values of greater than 1 are found in most areas in the eastern China. This implies that PM formation is most sensitive to changes in the emissions of SO_2 and is more sensitive to the emission reductions in NO_x than in NH_3. Such a sensitivity to PM precursors is consistent with results from four sensitivity simulations, each with a 50% reduction of emissions of four PM_{10} precursors including SO_2, NO_x, NH_3, and AVOCs in Jul. The sensitivity simulations indicate that reducing 50% of SO_2, NO_x, and NH_3 emissions leads to up to −27.8%, −25.0%, and −16.8% reduction of PM_{10} concentrations. Reducing 50% of AVOC emissions, however, leads to an increase by up to 8.8% in PM_{10} concentrations, due to increased formation of secondary inorganic aerosols.

As shown in the Part I paper, the model simulations at 36-km overpredict O_3 concentrations but underpredict those of SO_2, NO_x, and PM_{10}. These model biases and errors may affect process analysis results to some extent. For example, since the underpredictions in PM_{10} concentrations are mainly caused by the underestimation in emissions, the process contributions to PM_{10} formation rates from primary PM emissions and emissions of PM gaseous precursors such as SO_2 and NO_x may be underestimated. Nevertheless, the results from this study provide useful insights into the governing processes that control the fate and transport of key pollutants in China. They indicate that different emission control strategies for air quality improvement (separate or integrated NO_x or VOC emission control) should be taken during different seasons and over different regions in the future to effectively control ambient O_3 and PM_{10} air pollution. In addition to emission controls, meteorological variables and their changes will also affect air quality improvement. Model simulations accounting for both emission control and climate change will be needed to develop climate-friendly emission control strategies for air quality improvement in the future in China.

Acknowledgements

The authors thank Ping Liu at North Carolina State University, U. S. for her help in setting up process analysis based on the CB05 mechanism in CMAQ. This work was funded by the U. S. NSF Career Award, No. Atm-0348819 and Shandong University in China. The meteorological simulations were funded by China Scholarship Council at Shandong University in China and the U.S. NSF Career Award No. Atm-0348819 at NCSU. The emissions used for model simulations were funded by the U.S. EPA at ANL.

Appendix. Supplementary information

Supplementary information associated with this paper can be found, in the online version, at doi:10.1016/j.atmosenv.2010.03.036

References

Ansari, A.S., Pandis, S.N., 1998. Response of inorganic PM to precursor concentrations. Environmental Science and Technology 32, 2706–2714.

Byun, D.W., Ching, J.K.S., 1999. Science Algorithms of the EPA Models-3 Community Multiscale Air Quality (CMAQ) Modeling System, EPA/600/R-99/030. Office of Research and Development, U.S. Environmental Protection Agency, Washington, D.C.

Gonçalves, M., Jimenez-Guerrero, P., Baldasano, J.M., 2008. Contribution of atmospheric processes affecting the dynamics of air pollution in south-western Europe during a typical summertime photochemical episode. Atmospheric Chemistry and Physics Discussions 8, 18457–18497.

Hogrefe, C., Lynn, B., Rosenzweig, C., Goldberg, R., Civerolo, K., Ku, J.-Y., Rosenthal, J., Knowlton, K., Kinney, P.L., 2005. Utilizing CMAQ process analysis to understand the impacts of climate change on ozone and particulate matter. The 4th Annual CMAS Models-3 User's Conference, Sept. 26–28, 2005, Chapel Hill, NC.

Jang, J.C., Jeffries, H.E., Tonnesen, S., 1995. Sensitivity of ozone to model grid resolution-II. Detailed process analysis for ozone chemistry. Atmospheric Environment 29, 3101–3114.

Jiang, G., Lamb, B., Westberg, H., 2003. Using back trajectories and process analysis to investigate photochemical ozone production in the Puget Sound region. Atmospheric Environment 37, 1489–1502.

Kimura, Y., Mcdonald-Buller, E., Vizuete, W., Allen, D.T., 2008. Application of a Lagrangian process analysis tool to characterize ozone formation in Southeast Texas. Atmospheric Environment 42, 5743–5759.

Kwok, R., Fung, J.C.H., Huang, J.-P., Lau, A.K.H., Lo, J., Wang, Z., Qin, Y., 2005. Comparison of CMAQ and SAQM using process analysis for Hong Kong ozone episodes. The 4th Annual CMAS Models-3 User's Conference, Sept 26–28, Chapel Hill, NC.

Liu, P., Zhang, Y., Yu, S.C., Schere, K.L., Use of a process analysis tool for diagnostic study on fine particulate matter predictions in the U.S. Part II: process analyses and sensitivity simulations, Atmospheric Environment, in review.

Lu, C.-H., Chang, J.S., 1998. On the indicator-based approach to assess ozone sensitivities and emissions features. Journal of Geophysical Research 103, 3453–3462.

Meng, Z., Dabdub, D., Seinfeld, J.H., 1997. Chemical coupling between atmospheric ozone and particulate matter. Science 277, 116–119.

Pai, P., Vijayaraghavan, K., Seigneur, C., 2000. Particulate matter modeling in the Los Angeles Basin using SAQM-AERO. Journal of the Air and Waste Management Association 50, 32–42.

Seinfeld, J.H., Pandis, S.N., 2006. Atmospheric Chemistry and Physics: From Air Pollution to Climate Change. John Wiley and Sons, Inc., 1203 pp

Sillman, S., He, D.-Y., 2002. Some theoretical results concerning O_3-NO_x-VOC chemistry and NO_x-VOC indicators. Journal of Geophysical Research 107 (D22). doi:10.1029/2001JD001123.

Sillman, S., He, D.-Y., Cardelino, C., Imhoff, R.E., 1997. The use of photochemical indicators to evaluate ozone-NO_x-hydrocarbon sensitivity: case studies from Atlanta, New York, and Los Angeles. Journal of the Air & Waste Management Association 47, 642–652.

Sillman, S., 1995. The use of NO_y, H_2O_2, and HNO_3 as indicators for ozone-NO_x-hydrocarbon sensitivity in urban locations. Journal of Geophysical Research 100 (D7), 4175–4188.

Tonnesen, G.S., Dennis, R.L., 2000a. Analysis of radical propagation efficiency to assess ozone sensitivity to hydrocarbons and NO_x 1. Local indicators of instantaneous odd oxygen production sensitivity. Journal of Geophysical Research 105 (D7), 9213–9225.

Tonnesen, G.S., Dennis, R.L., 2000b. Analysis of radical propagation efficiency to assess ozone sensitivity to hydrocarbons and NO_x 2. Long-lived species as indicators of ozone concentration sensitivity. Journal of Geophysical Research 105 (D7), 9227–9241.

Tonse, S.R., Brown, N.J., Harley, R.A., Jin, L., 2008. A process-analysis based study of the ozone weekend effect. Atmospheric Environment 42, 7728–7736.

Wang, X., Carmichael, G., Chen, D., Tang, Y., Wang, T., 2005. Impacts of different emission sources on air quality during March 2001 in the Pearl River Delta (PRD) region. Atmospheric Environment 39, 5227–5241.

Xu, J., Zhang, Y.-H., Wei, W., 2006. Numerical study for the impacts of heterogeneous reactions on ozone formation in Beijing urban area. Advances in Atmospheric Sciences 23, 605–614.

Xu, J., Zhang, Y.-H., Fu, J.S., Zheng, S.-Q., Wang, W., 2008. Process analysis of typical summertime ozone episodes over the Beijing area. Science of the Total Environment 399, 147–157.

Yu, S., Mathur, R., Kang, D., Schere, K., Tong, D., 2009. A study of the ozone formation by ensemble back trajectory-process analysis using the Eta-CMAQ forecast model over the northeastern U.S. during the 2004 ICARPT period. Atmospheric Environment 43, 355–363.

Zhang, Y.-H., Shao, K.-S., Tang, X.-Y., Li, J.-L., 1998. The study of urban photochemical smog pollution in China. Acta Scientiarum Naturalium Universitatis Pekinensis 34 (2–1), 392–400 (in Chinese).

Zhang, Y., Vijayaraghavan, K., Seigneur, C., 2005. Evaluation of three probing techniques in a three-dimensional air quality model. Journal of Geophysical Research 110 (D02305), doi:10.1029/2004JD005248.

Zhang, Y., Vijayaraghavan, K., Wen, X.-Y., Snell, H.E., Jacobson, M.Z., 2009a. Probing into regional O_3 and PM pollution in the U.S., part I. A 1-year CMAQ simulation and evaluation using surface and Satellite Data. Journal of Geophysical Research 114 (D22304), doi:10.1029/2009JD011898.

Zhang, Y., Wen, X.-Y., Wang, K., Vijayaraghavan, K., Jacobson, M.Z., 2009b. Probing into regional O3 and PM pollution in the U.S., Part II. An examination of formation mechanisms through a process analysis technique and sensitivity study. Journal of Geophysical Research 114 (D22305), doi:10.1029/2009JD011900.